

# Muon Lifetime

Daniel Stefanian, Shay Yakobovich

School of Physics and Astronomy, Tel Aviv University, Tel Aviv, Israel

December 11, 2024

## Abstract

In this study, we measured the average lifetime of muons, specifically focusing on the lifetimes of both generic and negative muons, using a right circular cylindrical plastic scintillator. The observed average muon lifetime,  $\tau_{\text{observed}} \approx 2.15 \pm 0.17 \mu\text{s}$ , aligns closely with the known value of  $2.19 \pm 2.2 \cdot 10^{-6} \mu\text{s}$  (within  $0.24\sigma$ ). Additionally, the measured negative muon lifetime of  $\tau_- \approx 2.1 \mu\text{s}$  deviates by  $\sim 4.4\%$  from the expected value,  $2.19703 \pm 4 \cdot 10^{-5} \mu\text{s}$ , demonstrating consistency within experimental uncertainty.

## 1 Introduction

The muon ( $\mu$ ), a fundamental particle in the lepton family<sup>3</sup>, plays a crucial role in probing fundamental interactions and testing the accuracy of the Standard Model of particle physics. Muons are produced in high-energy processes, such as cosmic ray interactions in the atmosphere, and they decay primarily via the weak interaction<sup>4</sup>. In this experiment, the atmosphere serves as our muon source. The muon's lifetime, approximately  $2.2\mu\text{s}$ , is a well-established quantity<sup>3</sup> that provides insight into weak force properties and allows for cross-checks with theoretical predictions.

Negative muons ( $\mu^-$ ) exhibit a slightly different decay behavior due to their ability to interact with atomic nuclei before de-

caying, which affects their lifetime relative to positive muons<sup>3</sup>. Thus, a separate investigation of the negative muon's lifetime offers additional insights into atomic and subatomic interactions that influence decay processes.

In this study, we aimed to measure the average lifetime of muons, with a specific focus on the negative muon's lifetime, using a plastic scintillator detector. This detector, constructed from a right circular cylindrical scintillator within a black anodized aluminum tube, enabled efficient detection and analysis of muon decays. By comparing our measured lifetimes to established values, we assess the accuracy of our experimental methods and contribute to the broader understanding of muon behavior and decay.

## 2 Instrumentation setup and signal processing

The devices used to detect muons and record their dwell times are as follows:

- Photomultiplier tube (PMT) - consists of a photocathode, dynodes, and an anode. Incident photons on the photocathode are converted to photoelectrons through the photoelectric effect. These photoelectrons are then amplified across dynodes with increasing voltage to boost the signal.

In this setup, a plastic scintillator emits blue to near-UV light when a muon excites its molecules. This light is directed to the PMT, which releases photoelectrons. A high voltage (HV) applied to the PMT controls the gain. The PMT outputs a current pulse corresponding to photon count, which is processed by a two-stage amplifier for data collection.

- Two-stage amplifier - consists of an initial gain stage, typically using a transistor or operational amplifier, followed by a second stage for further amplification. This design maximizes overall gain and improves the signal-to-noise ratio.

The PMT generates a small voltage pulse from detected light, which is amplified in the first stage, then further boosted in the second. Each stage is adjustable to optimize performance. The final output, a larger voltage pulse retaining the original shape, is sent to a voltage comparator for threshold

checks. This amplification is crucial for accurately detecting low-intensity signals, aiding precise muon decay time measurements.

- Discriminator - serves as a voltage comparator that analyzes the amplified signal against a user-defined threshold. It includes a threshold (TH) control knob, allowing users to adjust the voltage to optimize sensitivity for different signal levels. When the signal exceeds the set threshold, a TTL (Transistor-Transistor Logic) output pulse is generated, indicating significant events such as muon interactions.

Adjusting the threshold is essential: a higher threshold may miss valid signals, while a lower one can increase noise and produce false triggers. Careful tuning is key for accurate muon decay measurements and reliable data collection. The TTL pulse then activates the FPGA timing circuit for further processing.

- FPGA timing circuit - implemented in an FPGA, this circuit is adaptable for various experimental requirements. It utilizes a high-frequency clock to ensure precise timing by counting intervals between TTL pulses from the discriminator.

Upon receiving the first pulse, the circuit starts counting clock cycles. If a second pulse arrives within a set time window, it stops counting and logs the interval. These intervals are then sent to a PC for analysis, contributing to a muon decay time histogram for muon lifetime calculations.

If no second pulse arrives within the window, the circuit resets after approximately 1 ms, blocking further measurements temporarily. Only intervals shorter than a threshold (e.g., 20  $\mu$ s) are recorded, focusing on relevant decay events and filtering out noise.

This instrumentation setup ensures highly sensitive and precise detection of muons and their decay times. By amplifying and filtering signals, while precisely timing each event, the system enables accurate muon lifetime measurements essential for studying decay dynamics and constructing reliable histograms for analysis.

### 3 Methodology and data analysis

The effective area of the cylindrical detector was first calculated to evaluate its capability in detecting atmospheric muons. Since muons arrive from various angles, not all incoming particles interact with the detector at optimal orientations. The cylindrical shape allows for detection primarily of particles arriving within specific angles relative to the detector's axis.

This was done by running a Monte-Carlo simulation of the detector and incoming particles in Python. By randomizing the azimuthal and polar angles, radius of the incoming particles and their total number, we were able to find a converging value for the effective area of the cylindrical detector, specifically its' lateral surface area.

Since the upper base of the cylindrical detector captures all muons passing through it, this area is fully effective, requiring no

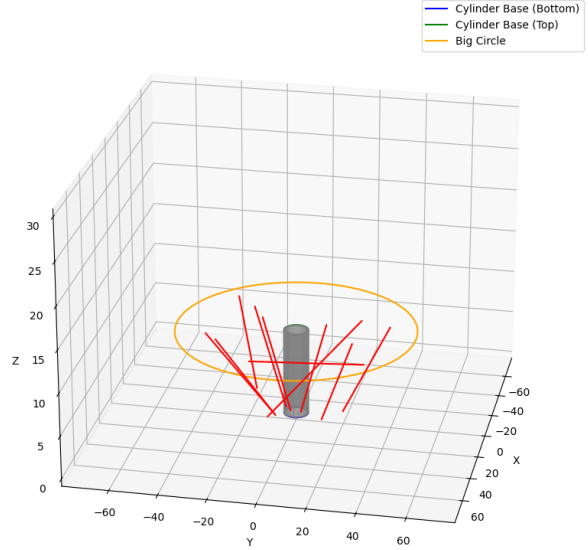


Figure 1: A Monte-Carlo simulation was performed to model randomized particle trajectories arriving at the detector, effectively simulating the incidence of muons.

additional simulation. The bottom base is excluded from calculations as muons entering through it would have already passed through the detector's active volume, making them irrelevant for additional detection. Hence, the total effective area of the detector is:

$$A_{tot} = A_{lateral\ eff} + A_{upper} \quad (1)$$

where  $A_{lateral\ eff}$  is the effective lateral surface area and  $A_{upper}$  is the upper base. The Monte-Carlo simulation outputs  $A_{lateral\ eff} \approx 1235\ cm^2$  as can be seen in Fig. 2. An analytical calculation is used to find the upper base area by using the radius of the detector  $r = 8.5 \pm 0.1\ cm$  which gives us  $A_{upper} = 2\pi r \approx 454 \pm 0.62\ cm^2$ . Using (1) and converting to meters, we get:

$$A_{tot} \approx 0.17 \pm 1.25 \cdot 10^{-4}\ m^2$$

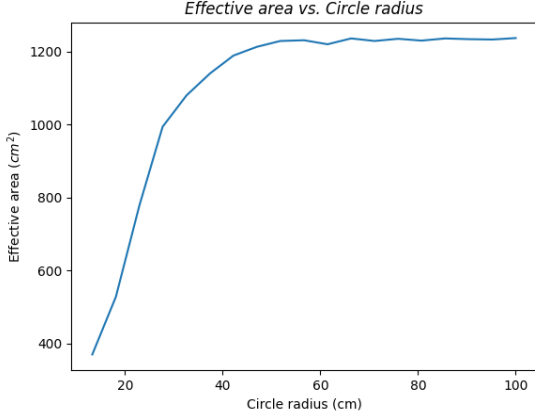


Figure 2: Effective area as a function of circle radius resulting from a Monte-Carlo simulation. Circle radius is a circular plane set right on top of the cylindrical detectors' upper base.

Then, the known muon flux (sea level) value<sup>1</sup>  $\phi_{measured} \approx 167 \text{ m}^{-2} \text{ s}^{-1}$  is used to calculate the expected muon count in our detector:

$$N_{expected} = A_{tot} \cdot \phi_{measured} \quad (2)$$

$$\approx 28.4 \pm 2.1 \cdot 10^{-2} \frac{\text{muon}}{\text{sec}}$$

To correctly evaluate the average lifetime of the muon  $\mu$ , a correct count of muon flux is needed. For that, it is crucial to set the optimal TH and HV values in the system. This optimization is done by taking multiple measurements of different TH and HV values and the signal count per 5 minutes, N. Doing this results in a dataset of TH, HV and N, for which an interpolation is applied using numerical tools.

By inputting the expected muon count N obtained from (2) into the interpolated function, we were able to derive the corre-

sponding threshold (TH) and high-voltage (HV) values:

$$TH \approx 0.85, HV \approx 1160$$

By using these optimized values, the system has been adjusted accordingly, and measurements of muons in the detector have now started. A dataset of muon counts and their time spent inside the detector until decay has been collected and sorted into a histogram. The first two bars of the histogram have been removed to minimize noise in the dataset. The histogram has then been divided into a signal region and a control region, as seen in Fig. 3:

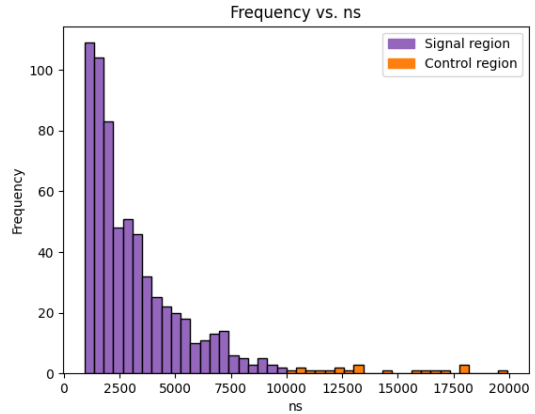


Figure 3: Muon count (frequency) as a function of time spent in the detector until decay in nanoseconds.

The division was done to enhance data analysis and interpretation. The signal region contains the events of interest — those muons that decay within the expected lifetime range. In contrast, the control region includes events that are outside the expected lifetime range, which helps to assess the background noise and other unrelated processes.

Using the histogram dataset from the control region, we can interpolate a periodic function that describes the noise in the system. The function is defined as:

$$y = A_0 \sin(kx + \delta) + C \quad (3)$$

where  $A_0$  is the amplitude of the periodic function,  $k$  the spatial frequency,  $\delta$  the phase shift and  $C$  the vertical offset. The interpolation optimizes the following parameters:

$$A_0 = 1 \text{ count } [\text{fixed}]$$

$$k = 1.91 \cdot 10^{-2} \pm 2.92 \cdot 10^{-4} \frac{\text{rad}}{\text{ns}}$$

$$\delta = -7.56 \cdot 10^{-1} \pm 4.29 \cdot 10^{-1} \text{ rad}$$

$$C = 1 \text{ count } [\text{fixed}]$$

with a  $\chi^2_{\text{reduced}}$  value of 1.07, which indicates a good fit. By using (3) along with these

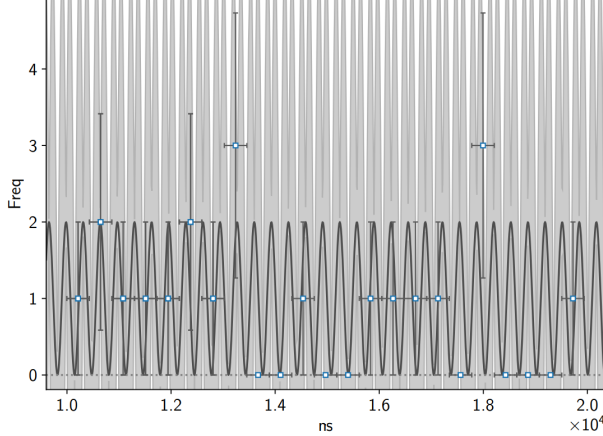


Figure 4: Sine function interpolation for the control region.

optimized parameters, we can subtract the noise from the signal region dataset and perform an additional interpolation in this region for an exponential function of the form:

$$y = A_1 e^{-\lambda x} + D \quad (4)$$

where  $A_1$  is the scaling factor,  $\lambda$  the decay rate and  $D$  is the vertical offset.

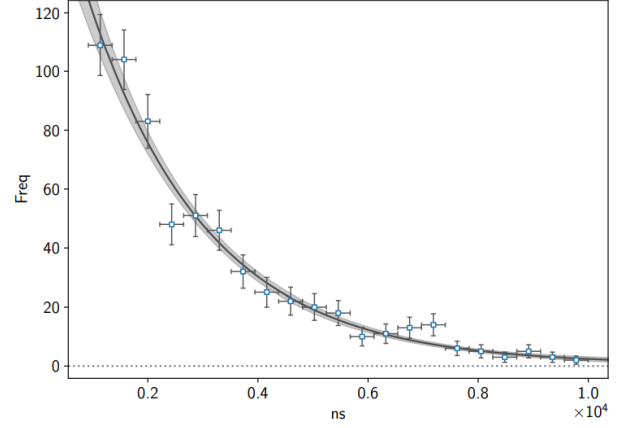


Figure 5: Exponential function interpolation for the signal region.

An additional interpolation gives the following optimized parameters:

$$A_1 = 1.9 \cdot 10^2 \pm 1.8 \cdot 10 \text{ count}$$

$$\lambda = 4.64 \cdot 10^{-4} \pm 3.7 \cdot 10^{-5} \frac{1}{\text{ns}}$$

$$D = 5.78 \cdot 10^{-1} \pm 1.11 \text{ count}$$

with a  $\chi^2_{\text{reduced}}$  value of 0.76, which, while not ideal, still provides a reasonable description of the data.

## 4 Results

After interpolation of the exponential function that describes the lifetime of muons, we can use the decay rate  $\lambda$  to estimate the average muon lifetime by using the simple relation:

$$\tau = \frac{1}{\lambda} \quad (5)$$

where  $\tau$  is the average muon lifetime. An additional analytical calculation of the error for the average lifetime is performed as

follows:

$$\sigma_\tau = \left| \frac{d\tau}{d\lambda} \right| \cdot \sigma_\lambda = \frac{1}{\lambda^2} \cdot \sigma_\lambda \quad (6)$$

where  $\sigma_\tau$  is the error for the average lifetime and  $\sigma_\lambda$  the error for the decay rate parameter  $\lambda$ . After the calculations, the **average muon lifetime** is:

$$\tau_{observed} \approx 2.15 \pm 0.17 \mu s$$

which is within  $0.24\sigma$  of the known measured value  $\tau_{measured} = 2.19 \pm 2.2 \cdot 10^{-6} \mu s$ .

Lastly, we derived the average negative muon ( $\mu^-$ ) lifetime  $\tau_-$  by using the following relation<sup>2</sup>:

$$\tau_{observed} = (1 + \rho) \frac{\tau_- \cdot \tau_+}{\tau_+ + \rho \cdot \tau_-} \quad (7)$$

where  $\rho$  is the ratio of the number of positive muons to the number of negative muons and  $\tau_+$  is the average lifetime of the positive muon ( $\mu_+$ ).

Since positive muons are not captured by the scintillator material nuclei<sup>5</sup>, we can approximate the average lifetime of the positive muon as the average free space muon lifetime value<sup>3</sup> of  $\tau_\mu \approx 2.197 \mu s$ . This, together with the known value of the ratio<sup>6</sup>  $\rho \approx 1.27$  and (7), allows us to calculate the **average negative muon lifetime** to be:

$$\tau_- \approx 2.1 \mu s$$

## 5 Discussion

The results of our experiment demonstrate a strong agreement with the established muon lifetime, reinforcing the reliability of our methodology and the effectiveness of

the cylindrical detector design. The observed average muon lifetime of  $\tau_{observed} \approx 2.15 \pm 0.17 \mu s$  is consistent with the known value, validating our data analysis techniques, including the Monte-Carlo simulations and noise filtering processes.

The observed deviation in the negative muon lifetime ( $\tau_- \approx 2.1 \mu s$ ) highlights the significant interactions of negative muons with material nuclei, which result in shorter lifetimes compared to their positive counterparts. This difference underscores the necessity for further studies to enhance our measurements and deepen our understanding of the unique decay processes and interactions of negative muons with matter.

Moreover, the division of the histogram into signal and control regions proved crucial in isolating the events of interest from background noise, enhancing the clarity of our findings. Future experiments could benefit from improved detector designs and more sophisticated data analysis techniques to further minimize noise and increase the precision of muon lifetime measurements.

Overall, our study contributes valuable insights into muon behavior and lays the groundwork for future research in particle physics.

## References

- [1] J.L. Autran, D. Munteanu, T. Saad Saoud, S. Moindjie,, *Characterization of atmospheric muons at sea level using a cosmic ray telescope*, Nuclear Instruments and Methods in Physics Research Section A: Accelerators, Spectrometers, Detectors and Associated Equipment, Volume 903, 2018, Pages 77-84, ISSN 0168-9002, <https://www.sciencedirect.com/science/article/abs/pii/S0168900218307599>
- [2] Coan, T.E., & Ye, J. , *Muon Physics*, New Jersey Institute of Technology, <https://www.njit.edu/>
- [3] PDG Group, *Progress of Theoretical and Experimental Physics*, Volume 2020, Issue 8, August 2020, 083C01, <https://doi.org/10.1093/ptep/ptaa104>
- [4] Klein, S. R. , *Muon Production in Relativistic Cosmic-Ray Interactions* , 2009, <https://arxiv.org/abs/0907.4799v2>
- [5] Feinberg, G., & Lederman, L. M., *The Physics of Muons and Muon Neutrinos*, Annual review of nuclear and particle science, Vol. 13:431-504, 1963
- [6] CMS Collaboration, *Measurement of the charge ratio of atmospheric muons with the CMS detector*, Physics Letters B, Volume 692, Issue 2, 23 August 2010, Pages 83-104, <https://www.sciencedirect.com/science/article/pii/S0370269310008725?via%3Dihub>